UCRL-JC-150223

A Methanol Steam Reforming Micro Reactor for Proton Exchange Membrane Micro Fuel Cell System

H. G. Park, W. T. Piggott, J. Chung, J. D. Morse
M. Havstad, C. P. Grigoropoulos, R. Greif, W. Benett,
D. Sopchak, R. Upadhye

This article was submitted to Hydrogen and Fuel Cells 2003 Conference and Trade Show, Vancouver, BC, Canada, June 8-11, 2003

July 28, 2003

U.S. Department of Energy
Lawrence Livermore National Laboratory

A METHANOL STEAM REFORMING MICRO REACTOR FOR PROTON EXCHANGE MEMBRANE MICRO FUEL CELL SYSTEM

Hyung Gyu Park[1], W. Thomas Piggott[2], Jaewon Chung[1], Jeffrey D. Morse[2], Mark Havstad[2], Costas P. Grigoropoulos[1], Ralph Greif[1], William Benett[2], David Sopchak[2], and Ravi Upadhye[2]

[1] Department of Mechanical Engineering, University of California at Berkeley, Berkeley, CA 94720
[2] Center for Micro and Nano Technology, Lawrence Livermore National Laboratory, Livermore, CA 94550

ABSTRACT

The heat, mass and momentum transfer from a fuel reforming packed bed to a surrounding silicon wafer has been simulated. Modeling showed quantitatively reasonable agreement with experimental data for fuel conversion efficiency, hydrogen production rate, outlet methanol mole fraction and outlet steam mole fraction. The variation in fuel conversion efficiency with the micro reformer thermal isolation can be used to optimize fuel-processing conditions for micro PEM fuel cells.

NOMENCLATURE

A, B	Pre-exponential term in Arrhenius expression for k [6]
C	Molar concentration (kmol/m^3)
c_p	Heat capacity (J/kg·K)
D	Mass diffusivity (m^2/s)
D_p	Catalyst particle size (m)
E	Activation energy in Arrhenius expression for k [6]
ΔH	Heat of reaction
k	1) Forward rate constant: prime means reverse (s^{-1} for reforming, and kmol/m^3 s for decomposition) 2) Thermal conductivity (W/m·K)
M	Molar weight (kg/kmol)
m	Mass fraction
P	Pressure (Pa)
$\dot{r}'''$	Rate of production (kmol/m^3·s)
$\overline{R}$	Gas constant: 8314 J/kmol K
SMR	Steam to methanol molar ratio
T	Temperature (K, °C)
u	Velocity vector (m/s)
w'''_{cat}	Catalyst density (kg$_{cat}$/m^3)
x	Mole fraction

Greek letter

ϵ	Porosity or void volume fraction
δ	Conversion Efficiency of decomposition
η	Conversion efficiency of reforming
μ	Molecular viscosity (kg/m·s)
ρ	Density (kg/m^3)
ξ	Reactor coordinate, along the channel (mm)
ξ^*	Nondimensionalized reactor coordinate, ξ / (u_{in} / k_R)

Subscripts

in, out	Property or variable at inlet and outlet, heat input (in)
i	Species index (1: CH_3OH, 2: H_2O, 3: H_2, 4: CO_2, 5: CO)
cat	Catalyst
req'd	Required heat
R	Reforming reaction, Reformer
D	Decomposition reaction
W	Water-gas shift reaction

INTRODUCTION

Modern work on fuel cells dates to at least the Gemini space program in the 1960s [1]. Miniature fuel cells have been worked recently for applicability to a wide range of portable devices: consumer electronics and portable field energy sources for military, for example [2].

For everyday portable usage, where high mobility and low operating temperature is required, PEMFCs (Proton Exchange Membrane Fuel Cell) have potential [1]. Hydrogen may be provided to the fuel cell from an existing hydrogen source, or by on-board generation. The on-board generation of hydrogen is preferred due to safety, distribution and fuel storage concerns. One of the on-board generation methods that can provide hydrogen stably is steam reforming. Since PEMFC and steam reforming have to be scaled down together as an integrated power system, MEMS techniques have many advantages [3].

Although all hydrocarbons can be steam reformed at suitable temperatures, methanol can be reformed at a significantly lower temperature than most other hydrocarbons (e.g., 300 °C for methanol vs. 600 °C for butane) [4,5]. In order to make methanol reforming the method of choice for supplying hydrogen to miniature fuel cells, a number of problems must be addressed. Among them are: CO generation and pressure drop across the reactor. Methanol reforming typically yields about 74% H2, 24% CO2 and 2% CO in the product. Since CO in concentrations above 100 ppm poisons the electrode catalysts, it is important to keep CO concentration as low as possible. Minimizing the pressure drop across the reactor is also important, since high pressure drops place more stringent requirements on fuel delivery system

MODELING OF THE REACTING FLOW IN A MICRO REFORMER

In the presence of catalyst ($CuO/ZnO/Al_2O_3$) and enough energy, the reforming, methanol decomposition, and water-gas shift reactions occur [6]:

$$CH_3OH + H_2O \underset{k_R'}{\overset{k_R}{\longleftrightarrow}} CO_2 + 3H_2 \quad \text{(reforming) (1)}$$

$$CH_3OH \xrightarrow{k_D} CO + 2H_2 \quad \text{(decomposition) (2)}$$

$$CO + H_2O \underset{k_W'}{\overset{k_W}{\longleftrightarrow}} CO_2 + H_2 \quad \text{(water-gas shift) (3)}$$

At the microscale the reforming occurs by a heterogeneous reaction but here in both TOPAZ3D [7,8] and FLUENT [9], the reactions were modeled as homogeneous in a packed bed (Figure 1).

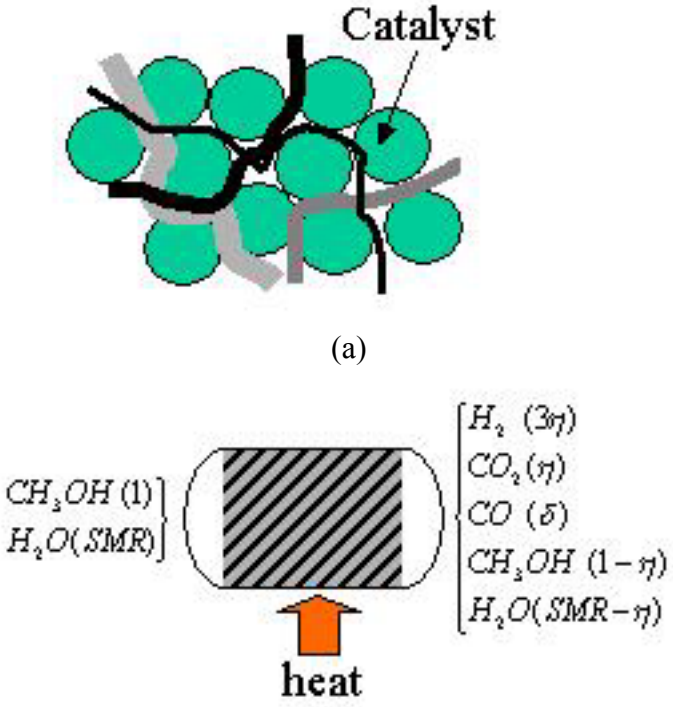

Figure 1. Schematic of modeling the micro reformer (a) microscopic point of view (b) macroscopic model

Reaction kinetics

Assuming the pressure drop is negligible system, the reaction kinetics can be represented as follows [6]:

$$\dot{r}_R''' = k_R C_1, \quad \dot{r}_D''' = k_D \qquad \text{(4a,b)}$$

$$k_R = \bar{k}_R w_{cat}''', \quad k_D = \bar{k}_D w_{cat}''' \qquad \text{(5a,b)}$$

$$\bar{k}_{\mathrm{R}} = \left[A_{\mathrm{R}} + B_{\mathrm{R}} \ln(\mathrm{SMR})\right] \exp\left[-\frac{E_{\mathrm{R}}}{\bar{R}T}\right] \quad (6)$$

$$\bar{k}_{\mathrm{D}} = A_{\mathrm{D}} \exp\left[-\frac{E_{\mathrm{D}}}{\bar{R}T}\right] \quad (7)$$

The mass of catalyst used in this calculation is 65mg.

Governing equations

In order to simulate the reacting flow with heat/mass transfer in the micro reformer, the following governing equations for mass and momentum conservation, energy transport, and species transport are solved:

$$\nabla \cdot (\rho \mathbf{u}) = 0, \quad (8)$$

$$\nabla \cdot (\rho \mathbf{u}\mathbf{u}) = \nabla \cdot \mu \nabla \mathbf{u} - \nabla p - \frac{150\mu(1-\varepsilon)^2}{\varepsilon^3 D_p^2}\mathbf{u}, \quad (9)$$

$$\nabla \cdot (\rho \mathbf{u} c_{\mathrm{p}} T) = \nabla \cdot k \nabla T - \Delta H_{\mathrm{R}} \dot{r}_{\mathrm{R}}''' - \Delta H_{\mathrm{D}} \dot{r}_{\mathrm{D}}''', \quad (10)$$

$$\nabla \cdot (\rho \mathbf{u} m_{\mathrm{i}}) = \nabla \cdot \rho D_{\mathrm{i}} \nabla m_{\mathrm{i}} + M_{\mathrm{i}} \dot{r}_{\mathrm{i}}''', \quad (11)$$

$$\rho = \frac{P}{\bar{R}T} M = \frac{P}{\bar{R}T} \sum_{\mathrm{i}} x_{\mathrm{i}} M_{\mathrm{i}}. \quad (12)$$

The material properties are determined as in the references [3,9].

Geometry and boundary condition

It is important to allow sufficient contact area and time between the catalyst and flow for the reforming reactions to take place. A serpentine microchannel reactor was used for this study, as this design fits a longer channel length into a more compact package. Figure 2 displays the micro fabricated reactor geometry and computational mesh with boundary conditions. To avoid computational complexity, detailed modeling of the two-phase evaporation region was neglected. Instead, the amount of heat required to evaporate the liquid is treated as a heat sink within the model. Therefore, the gas flow inlet starts after the evaporator heater at a temperature of 100°C. The inlet flow rate is set based on a 1.1:1 mole ratio of steam and methanol liquid flowing into the reformer at 10 μL/min (1.47×10^{-7} kg/s). At the outlet, a pressure boundary condition of 1 atm is applied. A constant heat flux is provided through the bottom of the reformer, simulating electrical heating. The no slip boundary condition is given at the reactor wall.

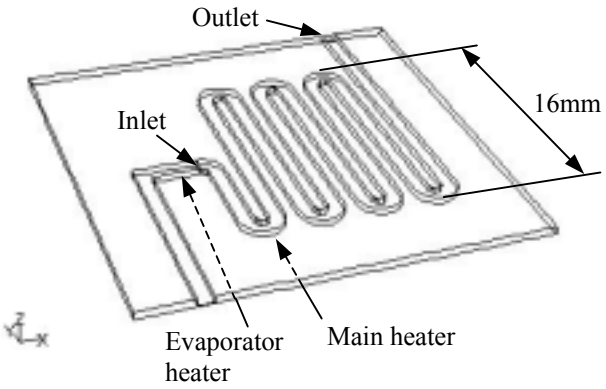

(a)

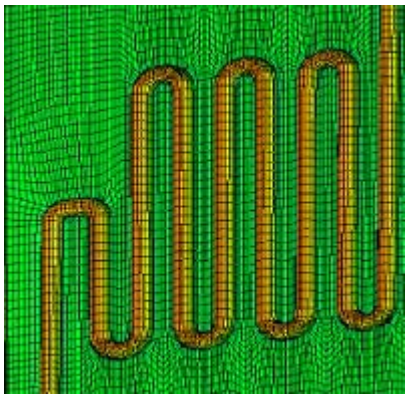

(b)

Figure 2. Geometry and mesh generation

Results: flow characteristics

The flow field modeled in this study is only perturbed from a straight channel flow at the U bends in the channel. As seen in Figure 3, the

velocity profile becomes non-uniform in the bends, accelerating at the inner and decelerating at the outer portion of the channel bend. This is due to the same pressure drop occurring at different flow path lengths between inner and outer curves.

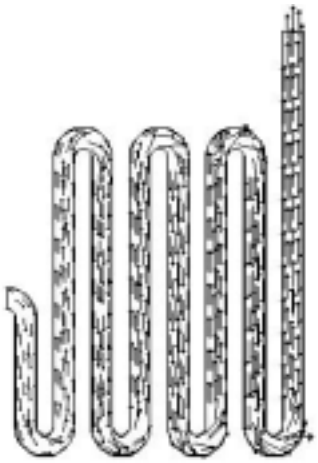

(a)

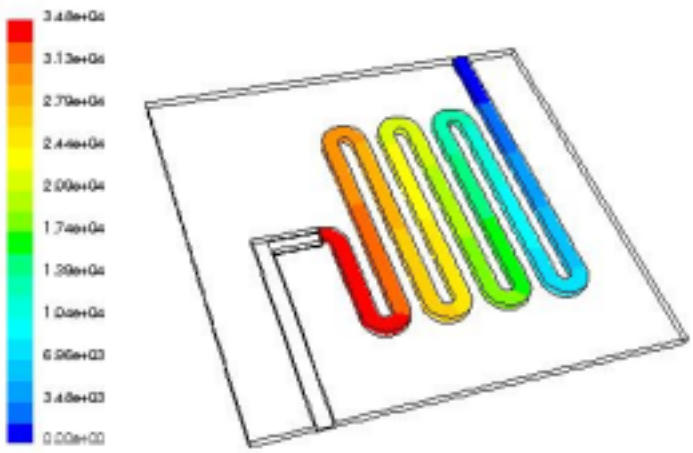

(b)

Figure 3. Flow characteristics:
(a) velocity field (b) pressure drop

Figure 4 shows the temperature field in the micro reformer. The temperature field across the chip appears relatively uniform (within 10° C) due to the relatively high thermal conductivity of the silicon wafer. For a micro reformer exposed to quiescent air at room temperature, the heat required to operate the reactor at 250°C was 3.5W.

The major mass transport behavior in the flow direction is the balance between the convection and source terms in eq. (11). At the curved regions in the serpentine micro channel, the convection term, $\rho \mathbf{u} m_i$, speeds up the mass transport in the inner portion of the channel bends. Therefore there appears a region in the flow where the species mole fraction (or concentration) profile becomes non-uniform across the channel. The mass diffusion term in the governing equations acts to smooth this non-uniform profile. Therefore, unlike a simple straight reactor, the mass diffusion term cannot be neglected in a complex geometry.

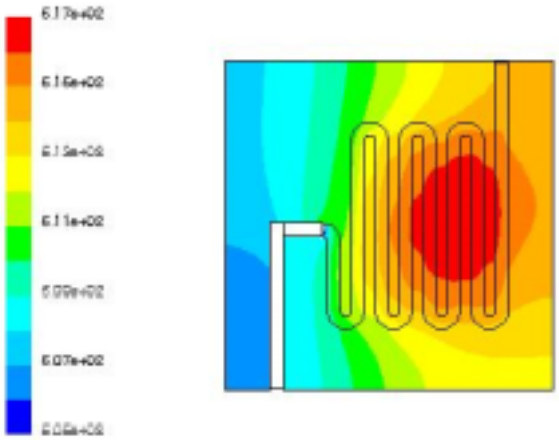

(a)

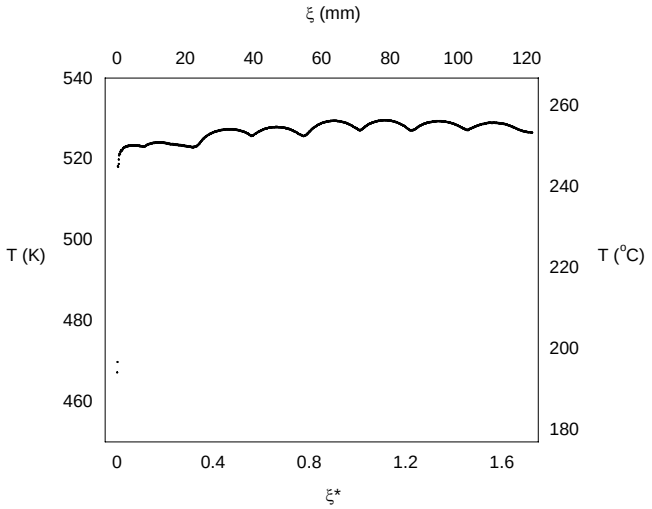

(b)

Figure 4. Temperature field

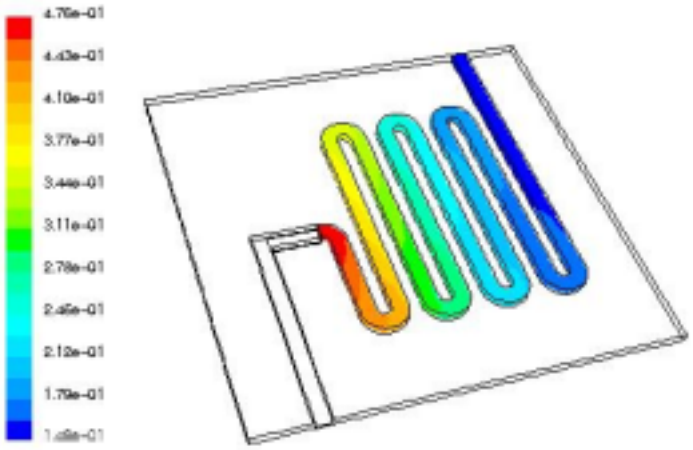

(a)

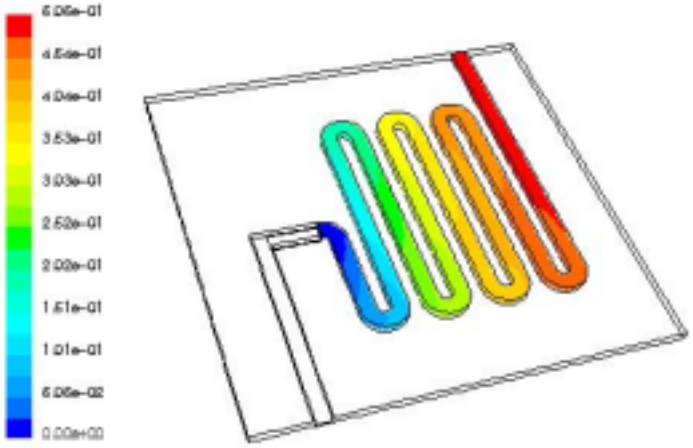

(b)

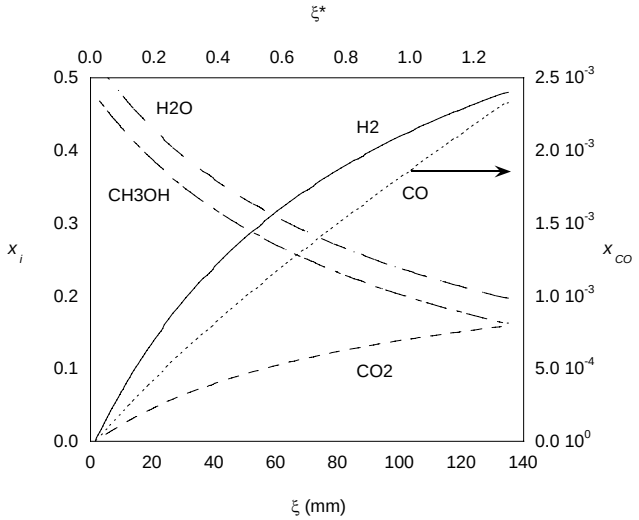

(c)

Figure 5. Species transport in a micro reformer: (a) the methanol (reactant) mole fraction, (b) hydrogen (product) mole fraction, (c) mean mole fractions of all the species in the reactor coordinate direction

Figure 5 displays both the initiation of the non-uniformities in species concentrations in the channel bends, and their reduction along the straight portion of the channel. It also shows the variation of the mole fraction of each species along the reactor, where a reactor coordinate along the length of the channel, ξ, has been defined.

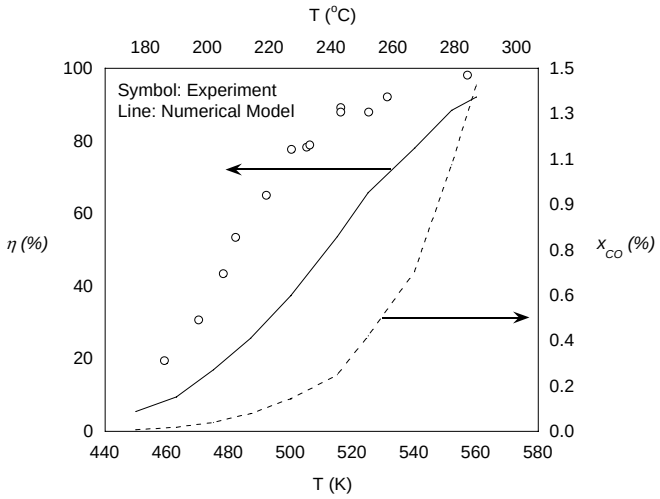

Figure 6. Variations of conversion efficiency and the CO mole fraction vs. the reformer temperature

Overall reactor performance, as measured by the conversion efficiency [3] and the amount of CO produced, are functions of temperature, due to the reaction kinetics. The conversion efficiency, determined below, is shown in Figure 6.

$$\eta = -1 + \frac{1}{x_1 + \frac{1}{2}} \qquad \text{(conversion efficiency)} \qquad (13)$$

This definition of the conversion efficiency is based on the stoichiometry of the reforming reaction, here labeled as reaction (1). For the specified flow rate, figure 6 shows that the reaction does not reach equilibrium conditions in the reactor at low temperatures. However, at high temperatures, the reaction can reach equilibrium for this flow rate. If we define a space-time as the amount (mass) of catalyst per a certain unit of the liquid flow rate, it is 6.5 mg·min/μL for this model.

The conversion efficiency shown in Figure 6 shows a shift off the experimental data [10]. One

reason could be the reaction kinetics. Amphlett *et al*. [6] presented their reaction kinetics results for temperatures less than 220°C, while the present temperature range is from 180 to 300°C. Another reason could be due to the catalyst preparation and placement in the reactor. Chung *et al*. [10] used crushed $CuO/ZnO/Al_2O_3$ catalyst in a packed bed. This method of preparation might have increased the real catalyst surface area in contact with the flow, providing more space over which the reactions could occur.

Figure 6 also shows the variation of the carbon monoxide mole fraction with respect to the reformer temperature. For this experiment, the rate of CO generation can be reduced by lowering the reaction temperature. However, this significantly decreases the hydrogen production as well because the reaction kinetics of hydrogen generation diminishes at temperatures near 200°C, so that a different CO control should be considered.

THERMAL DESIGN

Joule (I^2R) or combustion heating must be provided for: 1) reactant evaporation and heating, 2) the endothermic heat of reaction and 3) compensating for the conductive loss to the surroundings; the sum of the three must be only a small fraction of the device output. Here we consider joule heating applied between two reformer assemblies (Figure 7 shows half of a symmetrical insulation and reformer stack). Weak natural convection occurs at the outer surface of the housing with the surrounding air.

Assuming one-dimensional heat transfer, the heat loss from the reformer to the surroundings is obtained from:

$$q''_{\text{in}} = q''_{req'd} + q''_{\text{loss}},$$

$$q''_{\text{loss}} = \frac{T_{\text{R}} - T_{\infty}}{\frac{L}{k} + \frac{1}{h_{\infty}}} \qquad (14)$$

The heat loss is reduced when the conductive thermal resistance (L/k) becomes large, provided the reformer temperature is fixed, but practical size constraints restrict the thickness of the insulation. By fixing the heat flux and varying thermal resistance the reformer temperature (T_{R}) changes, which changes the reformer efficiency as shown in Figure 6.

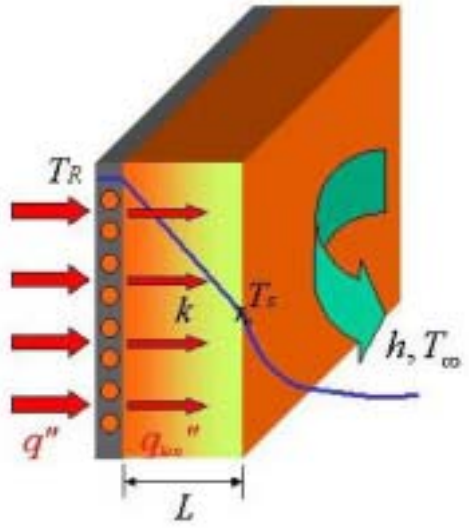

Figure 7 Schematic for simple insulation model

Thermal effects have also been simulated with the heat transfer code TOPAZ3D. The thermal conductivity and length of the insulation was varied to observe the effects of input heat flux and surface temperature on the operation of the reformer. The calculation used 77816 finite (solid conduction) elements and 137 axial plug flow reactor elements [8,9], with the same inlet conditions and amount of catalyst as in the FLUENT calculation. The left side of Fig. 7 is a symmetry plane, and thus specified as adiabatic (except for any joule heating imposed). The exterior of the insulation (the right hand side of fig. 7) cools by a natural convection with the surrounding fluid, air, at 300K. Mesh refinement was varied to ensure adequate discretization through the insulation.

Results

Figure 8 shows the relationship between the conductive thermal resistance, *L/k*, and the conversion efficiency of the reactor for a specified input heat flux. This result gives the insulation required to reach a desired reactor performance level. For example, polyimide foam, with a thermal conductivity of ~0.1W/m·K, must be 5cm thick to give a conversion efficiency of 80%. If an insulating material such as evacuated silica powder was used (with an effective conductivity of ~0.002W/m·K) the required insulation length is 1mm. Figure 8 may be used to select the thermal conductivity-insulation length pair to obtain a desired conversion efficiency for the current reformer.

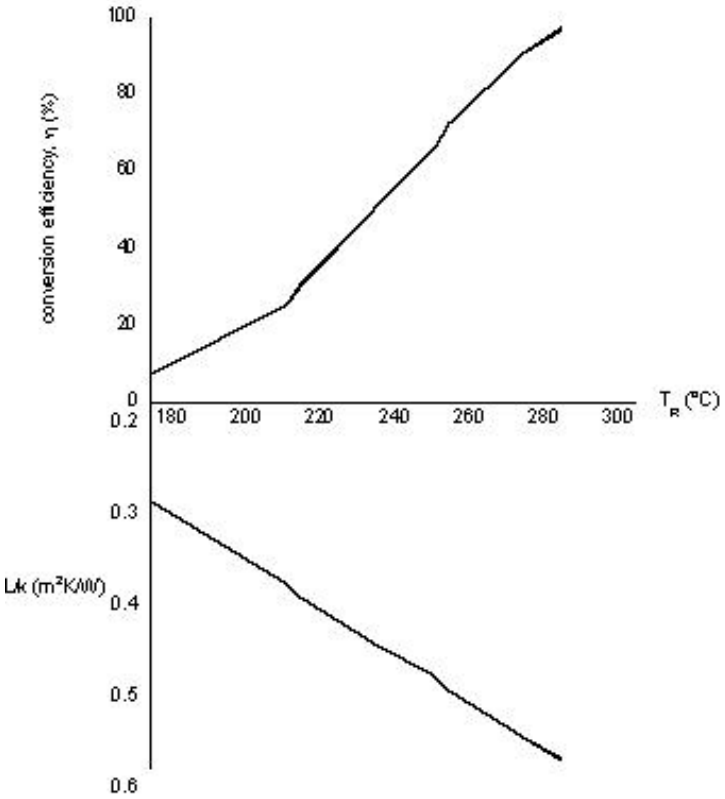

Figure 8**:** Conversion efficiency and L/k ratio for simple thermal model

An enhanced TOPAZ3D model has also been constructed and is being used to evaluate the three dimensional effects of adding side insulation to the model. Figure 9 shows a representative temperature profile for this model, with Figures 9(a) and (b) showing the heater and air side, respectively. About 100°C of temperature gradient was obtained for a 3mm layer of a polyimide foam with thermal conductivity *k*=0.046W/m·K. The heat input was 1.12W. This model will enable further evaluation of insulation effects on reformer performance.

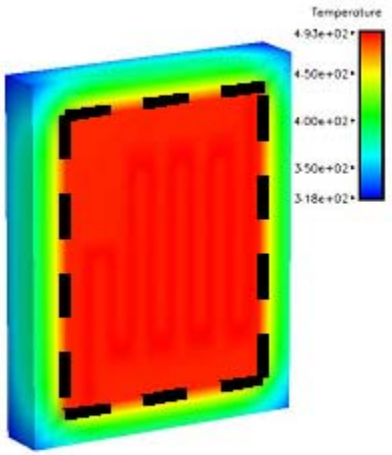

(a) Heater Side

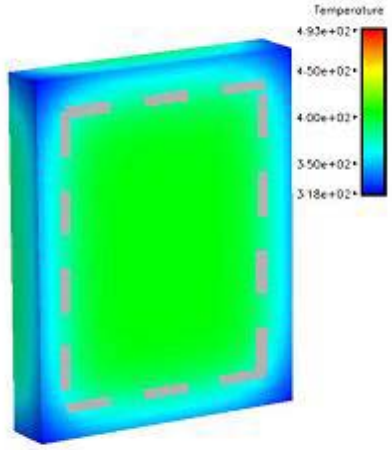

(b) Air side

Figure 9: Representative temperature profile for model with side insulation

CONCLUSIONS

The mass transport in a three-dimensional micro-reformer was characterized. The reaction source term affected the longitudinal transport, and the diffusion term affected the lateral transport. The temperature is fairly uniform throughout the reformer and wafer, due to the high thermal conductivity of silicon.

Setting the input heat flux, the relationship among area specific conductive thermal resistance, reformer temperature, and conversion efficiency was presented for use in selecting insulation material and thickness.

ACKNOWLEDGMENTS

This work was performed under the auspices of the U. S. Department of Energy by the University of California, Lawrence Livermore National Laboratory under Contract No. W-7405-Eng-48. The first author would like to acknowledge the support from the SEGRF (Student Employee Graduate Research Fellowship) program in the Lawrence Livermore National Laboratory. The third author would also like to acknowledge the support from the Campus Laboratory Exchange award in the University of California.

REFERENCES

1. J. St-Pierre, and D. P. Wilkinson. Fuel Cells: a New Efficient and Cleaner Power Source. *AIChE Journal*, 47(7), 1482-1486, July 2001.

2. J. D. Morse, A. F., Jankowski, R. T. Graff, and J. P. Hayes. Novel proton exchange membrane thin-film fuel cell for microscale energy conversion. *J. Vac. Sci. Technol. A*, 18(4), pp. 2003-2005, Jul/Aug 2000.

3. H. G. Park, J. Chung, C. P. Grigoropoulos, R. Greif, M. Havstad, and J. D. Morse. Transport in a microfluidic catalytic reactor. *Proceedings of 2003 ASME Summer Heat Transfer Conference*, Las Vegas, NV, USA, July 2003 (submitted)

4. L. F. Brown. A comparative study of fuels for on-board hydrogen production for fuel-cell-powered automobiles. *Int. J. Hydrogen Energy*, 26, pp. 381-397, 2001.

5. F. Joensen, and J. R. Rostrup-Nielsen. Conversion of hydrocarbons and alcohols for fuel cells. *J. Power Sources*, 105, pp. 195-201, 2002.

6. J. C. Amphlett, A. M. Creber, J. M. Davis, R. F. Mann, B. A. Peppley, and D. M. Stokes. Hydrogen production by steam reforming of methanol for polymer electrolyte fuel cells. *J. Hydrogen Energy*, 19(2), pp. 131-137, 1994.

7. A. B. Shapiro. *University of California, Lawrence Livermore National Laboratory, Rept. UCID-20484*, 1985.

8. M. Havstad. Surface Chemistry Effects in Finite Element Modeling of Heat Transfer in μ-Fuel Cells. *MSM* 2001. March 2001.

9. *Fluent User Guide v6*. Fluent Inc. 2001.

10. J. Chung, C. Harvey, M. Havstad, J. D. Morse, H. G. Park, D. Sopchak, and R. Upadhye. A microfluidic hydrogen generator for fuel cell applications. In AIChE annual meeting, San Francisco, CA, USA, Nov. 16-21, 2003. (submitted)

Hyung Gyu Park received the B.S. and M.S. degrees in mechanical engineering from the Seoul National University, Seoul, Korea in 1998 and 2000, respectively. He is a graduate student in mechanical engineering at the University of California, Berkeley and supported from the SEGRF program in the University of California, Lawrence Livermore National Laboratory. He is interested in micro fuel cells for portable applications.

W. Thomas Piggot received the B.S. and M.S. degrees in mechanical engineering from the University Illinois, Urbana-Champaign in 2000 and 2001, respectively. He is working in the University of California, Lawrence Livermore National Laboratory as a thermal fluids analyst. His research interest is modeling the thermal transport for micro fuel cells.

Jaewon Chung received the B.S. and M.S. degrees in mechanical engineering from the Yonsei University, Seoul, Korea and the Ph.D. degree from in mechanical engineering from the University of California, Berkeley in 1995, 1997 and 2002, respectively. Currently, he is a post doctorate in the University of California, Berkeley. His present research interests include laser diagnostics for microfluidic devices, laser curing of nano particle suspended solutions and micro fuel cells for portable applications.

Jeffrey D. Morse received the Ph.D. degree in electrical engineering from the Stanford University in 1992. He is currently an electrical engineer in the University of California, Lawrence Livermore National Laboratory. His research interests include the miniature fuel cell system design, micro technology based fabrication, MEMS, and Nano technology.

Mark Havstad received the B.S. degree in engineering and applied science from the Yale University in 1978, the M.S. degree in mechanical engineering from the Colorado State University in 1980, and the Ph.D. degree in mechanical engineering from the Stanford University in 1992. He is now working as a mechanical engineer in the University of California, Lawrence Livermore National Laboratory. He is interested in thermal analysis and code development.

Costas P. Grigoropoulos received his diploma degrees in naval architecture and marine engineering and in mechanical engineering from the National Technical University of Athens, Greece in 1978 and 1980, respectively. He received the M.S. and Ph.D. degrees in mechanical engineering from Columbia University in 1983 and 1986, respectively. He is currently a Professor in the Department of Mechanical Engineering at the University of California at Berkeley. His present research interests include laser materials processing and nano/micro-machining, the fundamental investigation of rapid change of phase transformations and ultra-fast laser interactions with materials, thin film crystal growth for the fabrication of high-definition flat panel displays and electronic devices, micro/nanofluidics, microscale energy conversion and fuel cells. He has conducted research at the Mechanical Engineering Sciences Laboratory of the Xerox Webster Research Center and the IBM Almaden Research Center. He is a Fellow of the American Society of Mechanical Engineers.

Ralph Greif received the B.S degree in mechanical engineering from the New York University in 1956, the M.S. degree in mechanical engineering from the University of California, Los Angeles in 1958 and the Ph.D. degree in mechanical engineering from Harvard University in 1962. He is currently a Professor in the Department of Mechanical Engineering, University of California, Berkeley. His present research interests include heat and mass transfer, micro scale transport, fuel cells, cooling at the chip level, materials processing/deposition, laser surface interactions, nuclear reactor safety, phase change, buoyancy transport, bio heat transfer, and reacting flows.

William Benett works as a senior associate engineer in mechanical engineering in the University of California, Lawrence Livermore National Laboratory. His current research interests include the MEMS device design and packaging.

David Sopchak received the B.A. degree in chemistry from the Cook College, Rutgers University in 1994, and the Ph.D. degree in electrochemistry from the Case Western Reserve University in 2001. He has worked on fuel cell, as a post doctorate, in the University of California, Lawrence Livermore National Laboratory.

Ravi Upadhye received the B.S. degree in chemical engineering from the IIT, Bombay, India in 1967, the M.S. degree in chemical engineering from the University of New Brunswick, Canada in 1969, and the Ph.D. degree in chemical engineering from the University of California, Berkeley in 1974. He works as a deputy materials program leader for energy and environment in the chemistry and chemical engineering division in the University of California, Lawrence Livermore National Laboratory. He is interested in the research related to catalyst and process design.